

Signature of Wave Chaos in Spectral Characteristics of Microcavity Lasers

メタデータ	言語: eng 出版者: 公開日: 2018-01-11 キーワード (Ja): キーワード (En): 作成者: メールアドレス: 所属:
URL	https://doi.org/10.24517/00049733

This work is licensed under a Creative Commons Attribution 3.0 International License.





Signature of Wave Chaos in Spectral Characteristics of Microcavity Lasers

Satoshi Sunada,¹ Susumu Shinohara,² Takehiro Fukushima,³ and Takahisa Harayama⁴

¹*Faculty of Mechanical Engineering, Institute of Science and Engineering,
Kanazawa University, Kakuma-machi Kanazawa, Ishikawa 920-1192, Japan*

²*NTT Communication Science Laboratories, NTT Corporation, 2-4 Hikaridai Seika-cho Soraku-gun, Kyoto 619-0237, Japan*

³*Department of Information and Communication Engineering, Okayama Prefectural University,
111 Kuboki Soja, Okayama 719-1197, Japan*

⁴*Department of Applied Physics, School of Advanced Science and Engineering,
Waseda University, 3-4-1 Okubo, Shinjuku-ku, Tokyo 169-8555, Japan*

(Received 26 February 2016; published 20 May 2016)

We report an experimental investigation on the spectra of fully chaotic and nonchaotic microcavity lasers under continuous-wave operating conditions. It is found that fully chaotic microcavity lasers operate in single mode, whereas nonchaotic microcavity lasers operate in multimode. The suppression of multimode lasing for fully chaotic microcavity lasers is explained by large spatial overlaps of the resonance wave functions that spread throughout the two-dimensional cavity due to the ergodicity of chaotic ray orbits.

DOI: [10.1103/PhysRevLett.116.203903](https://doi.org/10.1103/PhysRevLett.116.203903)

Various active devices ranging from musical instruments to lasers generate oscillating states with well-defined frequencies from the interplay between resonator geometry and an active nonlinear element [1–3]. Understanding and controlling the formation of such self-organized oscillating states is important in device physics and related applications. As a specific example, two-dimensional (2D) microcavity lasers have attracted considerable attention over the past decades [4–6]. Depending on the cavity shapes, they can exhibit a variety of lasing states through the interaction between the light field and active gain material [3]. The studies of 2D microcavity lasers have led to a wide range of applications, including low-threshold microlasers with unidirectional emission [7–13], low-coherence microlasers [14], and fast random signal generation [15]. Moreover, 2D microcavity lasers have served as a platform for experimentally addressing fundamental issues such as quantum or wave chaos in open systems [16–21] and non-Hermitian physics [22,23].

Both experimental and theoretical studies on 2D microcavity lasers with various cavity shapes have shown that the lasing emission patterns can be well characterized by a limited number of low-loss resonance modes (i.e., eigenmodes with low losses in passive cavities) [3–5]. These studies motivated research on the resonance characteristics of microcavities [6], and presented an interesting problem on the mechanism of mode selection, namely, which modes and how many of them can simultaneously lase for a given cavity shape and pumping condition. The mode selection is mainly due to nonlinear mode couplings (via gain materials) such as mode competition [24,25], i.e., lasing of some modes suppresses that of other modes. While mode competition and its resulting lasing phenomena have been actively studied by a nonlinear dynamical model [26–30] and a steady state *ab initio* laser theory [31,32], the effect

of the cavity shapes on the selection of lasing modes is still unclear.

In this Letter, we shed light on the effect of cavity shapes on the number of lasing modes by systematically investigating the lasing spectra of 2D semiconductor microcavity lasers under continuous-wave (cw) operating conditions. We focus on two 2D microcavities that are categorized as fully chaotic and nonchaotic cavities from a ray optics point of view [3], where all of the internal ray orbits are chaotic in the former and none of the ray orbits are chaotic in the latter. The lasing in fully chaotic cavities has been studied to some extent [14,33–39], however, experimental investigations on the lasing spectra have not yet been performed in detail, such as by changing the cavity sizes and degrees of deformation from a circular cavity and comparing the spectra with those of nonchaotic cavities. Our investigations reveal that lasers with fully chaotic cavities (hereafter referred to as fully chaotic cavity lasers) exhibit strong suppression of multimode lasing and operate in single mode regardless of the cavity size and deformation parameters, whereas lasers with nonchaotic cavities (nonchaotic cavity lasers) operate in multimode. This is the first experimental result that systematically reveals the relationship between cavity shapes and spectral characteristics, despite the fact that single mode emission in fully chaotic cavity lasers has been reported previously in the literature [30,33,34].

In this work, we focus on a specific shape of the fully chaotic cavity called the stadium [40], which is widely used for classical and quantum chaos studies. As shown in Fig. 1(a), the stadium cavity consists of two straight lines of length l and two half circles of radius R . We define the aspect ratio parameter $p = W/L$, where $W = 2R$ is the length of the minor axis and $L = 2R + l$ is the length of the major axis. For the nonchaotic cavity, we focus on the

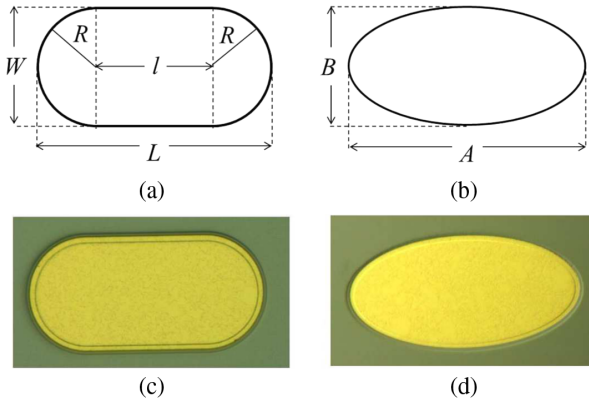


FIG. 1. (a) Stadium cavity and (b) elliptic cavity. (c),(d) Optical microscope images of the fabricated lasers, where both cavities have an area $S = 8748 \mu\text{m}^2$ and an aspect ratio $p = 0.5$.

elliptic cavity defined in Fig. 1(b). It is known that a closed elliptic cavity is an integrable system [41], thus exhibiting no chaotic behavior. In the same manner as for the stadium cavity, we define the aspect ratio parameter for the elliptic cavity as $p = B/A$, where A and B are the lengths of the major and minor axes, respectively.

We fabricated semiconductor microcavities with the stadium and elliptic cavities by applying a reactive-ion-etching technique to a graded index separate-confinement-heterostructure (GRIN-SCH) single-quantum-well GaAs/ $\text{Al}_x\text{Ga}_{1-x}\text{As}$ structure grown by metal-organic chemical-vapor deposition (MOCVD) (See Ref. [42] for details on the layer structures and fabrication process). The fabricated lasers are shown in Figs. 1(c) and 1(d). In our experiments, the lasers were soldered onto aluminum nitride submounts at $20 \pm 0.1^\circ\text{C}$ and electrically driven with cw current injection. The optical outputs were collected with anti-reflection-coated lenses and coupled to a multimode optical fiber via a 30-dB optical isolator.

Figure 2 shows the lasing spectra for the stadium cavity laser with a cavity area $S = 8748 \mu\text{m}^2$ and $p = 0.5$ ($R = 35 \mu\text{m}$ and $l = 70 \mu\text{m}$) for various current values above a threshold current $I_{\text{th}} \approx 74 \text{ mA}$. Because of the large area, the number of modes within the gain band was estimated to be a few thousand. Nevertheless, the lasing spectra exhibit only a single sharp peak regardless of the current value I . The peak continuously redshifts as I increases, due to a thermal effect. As shown in the inset of Fig. 2, the linewidth of the peak is approximately 0.004 nm , which is close to the resolution limit (0.002 nm) of our spectrum analyzer (Advantest Q8347). For further evidence on single-mode lasing (i.e., single-wavelength lasing), we measured the power spectrum of the output intensity using a photodetector with a bandwidth of 12.5 GHz and confirmed that there were no beat frequencies due to multimode lasing in the spectrum [30]. In addition, we evaluated the number of lasing modes by measuring the contrast of the far-field emission pattern [43]. Using a relationship between the contrast and the number of lasing modes [14], we obtained a result that suggested single-mode operation.

Figure 3 shows the lasing spectra of the elliptic cavity laser for various current values above $I_{\text{th}} \approx 34 \text{ mA}$ [44]. The area and aspect ratio of the elliptic cavity are same as those of the stadium cavity. As compared to Fig. 2, there is a remarkable difference in the appearance of multiple peaks. In order to quantify the difference of the spectral characteristics between the two lasers, we counted the number of lasing peaks whose intensities were larger than -20 dB of the maximum peak intensity in each spectrum. Figure 4 shows the number of peaks as a function of the current normalized by the threshold value I_{th} for each laser. As shown in Fig. 4, the difference in the number of peaks between the two lasers increases as I increases. We also investigated the spectral characteristics for various cavity areas with a fixed p value and found similar tendencies

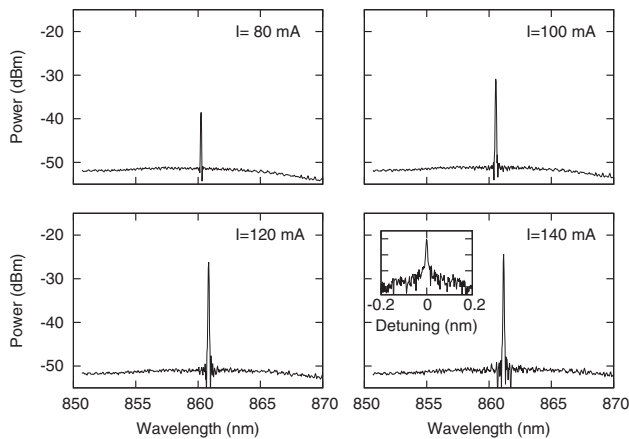


FIG. 2. Spectra of the stadium cavity laser with a cavity area $S = 8748 \mu\text{m}^2$ and an aspect ratio $p = 0.5$ for various current values. The threshold current is approximately 74 mA .

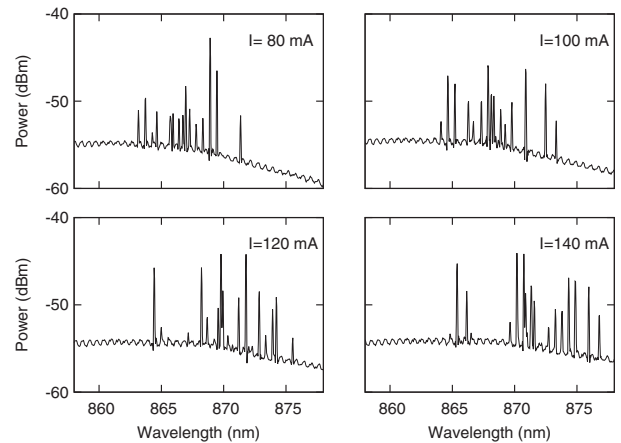


FIG. 3. Spectra of the elliptic cavity laser with a cavity area $S = 8748 \mu\text{m}^2$ and an aspect ratio $p = 0.5$ for various current values. The threshold current is approximately 34 mA .

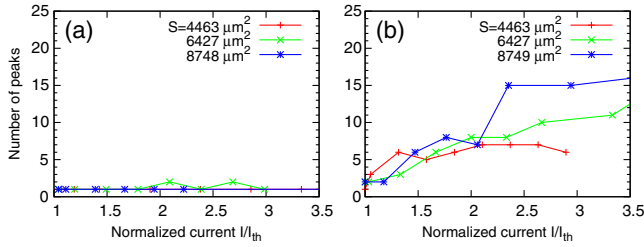


FIG. 4. Injection current dependence of the number of peaks in the spectra of (a) the stadium cavity lasers and (b) the elliptic cavity lasers with various cavity areas S . In both (a) and (b), the aspect ratio is $p = 0.5$.

toward a single-mode lasing state for the stadium cavity lasers and toward a multimode lasing state for elliptic cavity lasers. As a slight exception, we observed two peaks for the stadium cavity laser for $I/I_{th} = 2.1$ and 2.7 in Fig. 4(a). We attribute this to mode hopping caused by a thermal effect of the current injection, such as a gain shift and a change in the refractive index.

Even when changing the aspect ratios of the cavities, we found similar spectral characteristics. Figure 5(a) shows the current dependence of the number of peaks for the stadium cavity lasers with various p values, where the radius R is fixed at $25 \mu\text{m}$. The results for the elliptic cavity lasers with various p -values are shown in Fig. 5(b). $p = 1$ corresponds to a circular cavity, which is categorized as a nonchaotic cavity. There is a possibility that the number of peaks has been underestimated because some modes have such weak outputs (due to high confinement) that they cannot be captured in the far field. With a deformation toward the stadium shape (i.e., $p < 1$), the number of peaks decreases and single-mode lasing can be achieved for high current values [Fig. 5(a)]. On the other hand, a deformation toward an ellipse does not exhibit a transition to single-mode lasing and maintains a multimode lasing state [Fig. 5(b)].

The above results indicate that strong suppression of multimode lasing is a common feature of stadium cavity lasers. As discussed in Refs. [24,25], a competitive interaction occurs among modes that are overlapped not

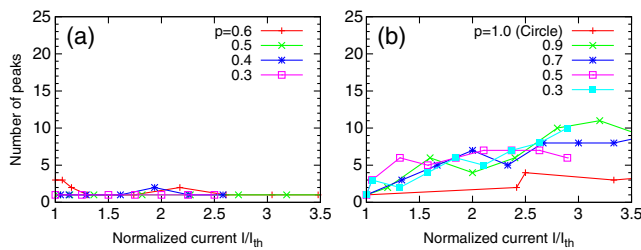


FIG. 5. Injection current dependence of the number of peaks in the spectra of (a) the stadium cavity lasers and (b) the elliptic cavity lasers with various aspect ratios p . In (a), the radius R is fixed as $25 \mu\text{m}$, (i.e., the area for $p = 0.5$ is $S = 4463 \mu\text{m}^2$). In (b), the areas of the elliptic cavities are the same as that of the stadium cavity with $p = 0.5$.

only spectrally but also spatially. In a fully chaotic cavity, modes typically have complex spatial patterns that spread throughout the entire cavity due to the ray dynamical property [for a typical example, see Fig. 6(a)], and therefore result in large spatial overlaps with other modes. Actually, previous numerical simulations of stadium cavity lasers demonstrated a strong selection of lasing modes owing to a competitive interaction [27,28,30]. Moreover, a frequency-locking phenomenon could occur and integrate several lasing modes into a single lasing mode [27,29,30]. On the other hand, nonchaotic cavities typically support spatially localized modes, e.g., whispering-gallery modes in circular and elliptic cavities. When modes are spatially localized in different areas, as shown in Figs. 6(c) and 6(d), and the spatial overlap is small, the competition among different modes can be avoided. Indeed, the simultaneous lasing of multiple whispering-gallery modes for a circular cavity laser was numerically demonstrated in Ref. [45].

The above discussion suggests that spatial modal overlapping is a necessary condition for modal interactions that suppress simultaneous lasing. To quantify the spatial overlaps between two modes, we introduce the following cross-correlation for the amplitude distributions of resonance modes:

$$C = \frac{\int |\phi(\mathbf{r})| |\psi(\mathbf{r})| w(\mathbf{r}) d\mathbf{r}}{\sqrt{(\int |\phi(\mathbf{r})|^2 w(\mathbf{r}) d\mathbf{r})(\int |\psi(\mathbf{r})|^2 w(\mathbf{r}) d\mathbf{r})}}, \quad (1)$$

where $\phi(\mathbf{r})$ and $\psi(\mathbf{r})$ are the modal wave functions and $w(\mathbf{r})$ represents a pumping region. For uniform pumping, $w(\mathbf{r}) = 1$ inside the cavity, whereas $w(\mathbf{r}) = 0$ outside. The correlation is essentially similar to a spatial contribution to the cross-gain saturation (i.e., intensity cross-correlation) between two modes [24,25,46]. Using the boundary element method [47], we calculated the resonances of the stadium and elliptic cavities with $p = 0.5$, imposing a refractive index of 3.3 inside the cavities and transverse

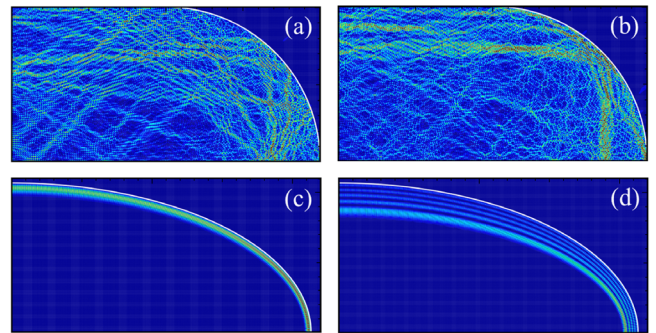


FIG. 6. (a),(b) Spatial intensity patterns of low-loss modes in a quarter of the stadium cavity, where (b) is a scarred mode with localization along a rectangular ray orbit. (c),(d) Spatial intensity patterns of whispering-gallery modes in a quarter of the elliptic cavity, where the radial mode number is $n_r = 1$ for (c) and $n_r = 5$ for (d).

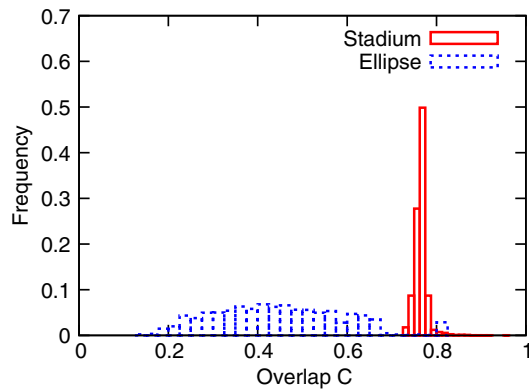


FIG. 7. Histogram of overlap C defined by Eq. (1) between two low-loss modes for the stadium cavity (solid) and elliptic cavity (dotted).

electric (TE) polarization. Because of computational power limitations, we set a size parameter $2\pi R/\lambda \approx 100$, where R and λ are the characteristic radius and wavelength, respectively. This size parameter value is smaller than that of a real laser cavity used in the experiments but is sufficiently large to discuss the properties of the wave functions in the short-wavelength regimes [35]. We obtained approximately 100 low-loss modes with a quality factor $Q \geq 3000$ for the stadium cavity, whereas $Q \geq 3 \times 10^5$ for the elliptic cavity. Figure 7 shows the histogram of the spatial overlap C between two low-loss modes for the two cavities. The C values for the stadium cavity are distributed around 0.77. It is known that several low-loss modes in chaotic cavities are so-called scarred modes [36,37] whose intensities are localized along unstable periodic ray orbits [e.g., see Fig. 6(b)]. An interesting finding is that there is a large overlap ($C \approx 0.73$) even for scarred modes. This can be explained by the fact that the localization of the scarred modes is generally weak and significant intensities are spread throughout the cavity.

In contrast, the C values for the elliptic cavity are widely distributed with a mean value of 0.45. The relatively low C values come from the small spatial overlaps between the localized modes. In particular, the overlaps are small between two modes with different radial mode numbers n_r , which characterize the number of field maxima in the radial direction. For instance, the C value between the modes with $n_r = 1$ [Fig. 6(c)] and $n_r = 5$ [Fig. 6(d)] is only 0.14. As seen in Fig. 3, the lasing peaks in the spectra of the elliptic cavity laser are not always equally spaced. This result means that modes with different n_r values were involved in the lasing, which supports our interpretation of the relation between the spatial overlaps and the spectral characteristics.

Lastly, we emphasize that the difference in the spectral characteristics between the stadium and elliptic cavity lasers was observed under the cw operating condition. Under this condition, single-mode lasing has also been

reported for other chaotic cavities with different shapes and different gain materials [33,34]. However, under pulsed operating conditions, multimode emission can be observed even for fully chaotic cavity lasers [14,35–39]. For example, in Ref. [30], multimode lasing has been observed in a stadium cavity laser for a pumping pulse width of $\lesssim 100 \mu\text{s}$ (see Fig. 11 of Ref. [30] for details). The result can be partially attributed to transient slow mode dynamics towards a steady lasing state [30].

In summary, we experimentally investigated the difference in the spectral characteristics between fully chaotic cavity lasers with a stadium shape and nonchaotic cavity lasers with an elliptic shape under the cw operating condition. In the stadium cavity lasers, only a single mode was excited at high pumping regimes regardless of the size and aspect ratio, whereas many modes were excited in the elliptic cavity lasers. The strong suppression of multimode lasing observed in the stadium cavity lasers can be explained by the large spatial overlaps among the low-loss modes. Because it is a common feature of fully chaotic cavities that the modal pattern spreads throughout the cavities, we expect that the modal suppression leading to single-mode lasing is a universal feature of fully chaotic cavity lasers.

The authors would like to gratefully acknowledge Professor A. D. Stone and Professor H. Cao for fruitful discussions and insightful comments. This work was partially supported by JSPS KAKENHI Grant No. 26790056.

-
- [1] T. Idogawa, T. Kobata, K. Komuro, and M. Iwaki, *J. Acoust. Soc. Am.* **93**, 540 (1993); M. E. McIntyre, R. T. Schumacher, and J. Woodhouse, *J. Acoust. Soc. Am.* **74**, 1325 (1983).
 - [2] H. Haken, *Synergetics. An Introduction, Nonequilibrium Phase Transitions and Self-organization in Physics, Chemistry, and Biology* (Springer, Berlin, 1977).
 - [3] T. Harayama and S. Shinohara, *Laser Photonics Rev.* **5**, 247 (2011).
 - [4] J. U. Nöckel and A. D. Stone, *Nature (London)* **385**, 45 (1997).
 - [5] C. Gmachl, F. Capasso, E. E. Narimanov, J. U. Nöckel, A. D. Stone, J. Faist, D. L. Sivco, and A. Y. Cho, *Science* **280**, 1556 (1998).
 - [6] H. Cao and J. Wiersig, *Rev. Mod. Phys.* **87**, 61 (2015).
 - [7] J. Wiersig and M. Hentschel, *Phys. Rev. Lett.* **100**, 033901 (2008).
 - [8] C. Yan, Q. J. Wang, L. Diehl, M. Hentschel, J. Wiersig, N. Yu, C. Pflügl, F. Capasso, M. A. Belkin, T. Edamura, M. Yamanishi, and H. Kan, *Appl. Phys. Lett.* **94**, 251101 (2009).
 - [9] Q. Song, W. Fang, B. Liu, S.-T. Ho, G. S. Solomon, and H. Cao, *Phys. Rev. A* **80**, 041807(R) (2009).
 - [10] C.-H. Yi, M.-W. Kim, and C.-M. Kim, *Appl. Phys. Lett.* **95**, 141107 (2009).

- [11] Q. J. Wang, C. Yan, N. Yu, J. Unterhinninghofen, J. Wiersig, C. Pflügl, L. Diehl, T. Edamura, M. Yamanishi, H. Kan, and F. Capasso, *Proc. Natl. Acad. Sci. U.S.A.* **107**, 22407 (2010).
- [12] G. D. Chern, H. E. Türeci, A. D. Stone, R. K. Chang, M. Kneissl, and N. M. Johnson, *Appl. Phys. Lett.* **83**, 1710 (2003).
- [13] X.-F. Jiang, C.-L. Zou, L. Wang, Q. Gong, and Y.-F. Xiao, *Laser Photonics Rev.* **10**, 40 (2016).
- [14] B. Redding, A. Cerjan, X. Huang, M. L. Lee, A. D. Stone, M. A. Choma, and H. Cao, *Proc. Natl. Acad. Sci. U.S.A.* **112**, 1304 (2015).
- [15] S. Sunada, T. Fukushima, S. Shinohara, T. Harayama, K. Arai, and M. Adachi, *Appl. Phys. Lett.* **104**, 241105 (2014).
- [16] H. G. L. Schwefel, N. B. Rex, H. E. Türeci, R. K. Chang, A. D. Stone, T. B. Messaoud, and J. Zyss, *J. Opt. Soc. Am. B* **21**, 923 (2004).
- [17] S. Shinohara and T. Harayama, *Phys. Rev. E* **75**, 036216 (2007).
- [18] S.-B. Lee, J. Yang, S. Moon, J.-H. Lee, K. An, J.-B. Shim, H.-W. Lee, and S.-W. Kim, *Phys. Rev. A* **75**, 011802(R) (2007).
- [19] G. Hackenbroich and J. U. Nöckel, *Europhys. Lett.* **39**, 371 (1997).
- [20] S. Shinohara, T. Harayama, T. Fukushima, M. Hentschel, T. Sasaki, and E. E. Narimanov, *Phys. Rev. Lett.* **104**, 163902 (2010); S. Shinohara, T. Harayama, T. Fukushima, M. Hentschel, S. Sunada, and E. E. Narimanov, *Phys. Rev. A* **83**, 053837 (2011).
- [21] S.-B. Lee, J.-H. Lee, J.-S. Chang, H.-J. Moon, S. W. Kim, and K. An, *Phys. Rev. Lett.* **88**, 033903 (2002).
- [22] M. Liertz, L. Ge, A. Cerjan, A. D. Stone, H. E. Türeci, and S. Rotter, *Phys. Rev. Lett.* **108**, 173901 (2012); M. Brandstetter, M. Liertz, C. Deutsch, P. Klang, J. Schöberl, H. E. Türeci, G. Strasser, K. Unterrainer, and S. Rotter, *Nat. Commun.* **5**, 4034 (2014).
- [23] B. Peng, S. K. Özdemir, S. Rotter, H. Yilmaz, M. Liertz, F. Monifi, C. M. Bender, F. Nori, and L. Yang, *Science* **346**, 328 (2014).
- [24] M. Sargent III, M. O. Scully, and W. E. Lamb, Jr, *Laser Physics* (Addison-Wesley, Reading, MA, 1974).
- [25] M. Sargent III, *Phys. Rev. A* **48**, 717 (1993).
- [26] T. Harayama, P. Davis, and K. S. Ikeda, *Phys. Rev. Lett.* **90**, 063901 (2003).
- [27] S. Sunada, T. Harayama, and K. S. Ikeda, *Phys. Rev. E* **71**, 046209 (2005).
- [28] T. Harayama, S. Sunada, and K. S. Ikeda, *Phys. Rev. A* **72**, 013803 (2005).
- [29] T. Harayama, T. Fukushima, S. Sunada, and K. S. Ikeda, *Phys. Rev. Lett.* **91**, 073903 (2003).
- [30] S. Sunada, T. Fukushima, S. Shinohara, T. Harayama, and M. Adachi, *Phys. Rev. A* **88**, 013802 (2013).
- [31] H. E. Türeci, A. D. Stone, and B. Collier, *Phys. Rev. A* **74**, 043822 (2006).
- [32] L. Ge, Y. D. Chong, and A. D. Stone, *Phys. Rev. A* **82**, 063824 (2010).
- [33] R. Audet, M. A. Belkin, J. A. Fan, B. G. Lee, K. Lin, F. Capasso, E. E. Narimanov, D. Bour, S. Corzine, J. Zhu, and G. Höfler, *Appl. Phys. Lett.* **91**, 131106 (2007).
- [34] M.-W. Kim, C.-H. Yi, S. Rim, C.-M. Kim, J.-H. Kim, and K.-R. Oh, *Opt. Express*, **20**, 13651 (2012).
- [35] S. Shinohara, T. Fukushima, and T. Harayama, *Phys. Rev. A* **77**, 033807 (2008).
- [36] T. Harayama, T. Fukushima, P. Davis, P. O. Vaccaro, T. Miyasaka, T. Nishimura, and T. Aida, *Phys. Rev. E* **67**, 015207(R) (2003).
- [37] W. Fang, H. Cao, and G. S. Solomon, *Appl. Phys. Lett.* **90**, 081108 (2007).
- [38] M. Lebental, J. S. Laurel, R. Hierle, and J. Zyss, *Appl. Phys. Lett.* **88**, 031108 (2006).
- [39] M. Choi, S. Shinohara, and T. Harayama, *Opt. Express* **16**, 17554 (2008).
- [40] L. A. Bunimovich, *Commun. Math. Phys.* **65**, 295 (1979).
- [41] M. V. Berry, *Eur. J. Phys.* **2**, 91 (1981).
- [42] T. Fukushima and T. Harayama, *IEEE J. Sel. Top. Quantum Electron.* **10**, 1039 (2004).
- [43] The contrast was defined as the standard deviation of the emission intensity divided by its mean value because the intensity exhibited a negative exponential distribution. The definition of the contrast is similar to that reported in Ref. [14].
- [44] The threshold current for the elliptic cavity laser was lower than that for the stadium cavity laser with the same area and aspect ratio. This can be explained by the fact that the elliptic cavity has high- Q whispering gallery modes (see Fig. 6).
- [45] S. Sunada, T. Harayama, and K. S. Ikeda, *Nonlinear Phenom. Complex Syst.* **10**, 1 (2007).
- [46] M. Yamada, *IEEE J. Quantum Electron.* **19**, 1365 (1983).
- [47] J. Wiersig, *J. Opt. A* **5**, 53 (2003).